Accurate analytic off-axis electron trajectories in realistic two-dimensional transverse wigglers with arbitrary magnetic field variation

P. Torggler and C. Leubner
Institut für Theoretische Physik, Universität Innsbruck, A-6020 Innsbruck, Austria
(Received 6 July 1988)

For several reasons, it is essential to have analytic descriptions of single-electron trajectories for wigglers and undulators. (a) They give a better insight into the complicated dependence of the electron motion on quantities like the injection conditions or the wiggler parameter K; (b) one can hope to calculate the radiation pattern from a particular wiggler or undulator only if at least the single-electron velocity is given in closed form; (c) analytic single-particle trajectories are an essential starting point for investigating advanced problems like stability analyses and free-electron laser performance. Therefore, single-electron motion was studied in wigglers with two-dimensional magnetic fields that are transverse and periodic but otherwise arbitrary on axis, and satisfy Maxwell's equations off axis. In this class of fields, the energy and one component of the canonical momentum are conserved and can be used to reduce the trajectory problem to the integration of a single complicated second-order ordinary differential equation, which, for all realistic electron-beam emittances and for all realistic values of $\delta_w = K/\gamma$, is weakly nonlinear and lends itself to a two-level two-scale analysis, through which an accurate analytic description of the complete electron trajectory can be established. This analytic trajectory exhibits all the features that one expects to find in off-axis motion, such as small-amplitude rapid wiggler oscillations superimposed on large-amplitude slowly varying betatron oscillations. The accuracy of this analytic trajectory was tested for a sinusoidal on-axis field variation by comparison with a numerical trajectory, and it was found that even for far-off-axis electrons, the agreement was excellent, typically on the order of one part in a thousand. This high accuracy in the off-axis regime is an important feature, since in many devices real transverse beam dimensions, initial beam velocity spreads, lateral beam injection, and a small undulator period λ_0 lead to electrons traveling considerably off axis.

I. INTRODUCTION

Wigglers and undulators are important for shaping the properties of synchrotron radiation to particular spectroscopic needs, and as major components of free-electron lasers (FEL's). So far, a large number of different magnetic field configurations have been studied. The "linear" or "transverse" wiggler—as opposed to the "helical" wiggler—is characterized by a median plane of symmetry (x-z plane in Fig. 1), which contains the wiggler axis (z axis in Fig. 1). In the median plane, the static magnetic field is everywhere perpendicular to this plane, and varies periodically along the wiggler axis.

Outside the median plane (i.e., off axis), the magnetic field is often approximated by the field on the wiggler axis.[1–4] Although such a field violates Maxwell's equations, it can nevertheless be regarded as a good approximation for electrons traveling sufficiently close to the wiggler axis. However, in almost all wiggler or undulator devices a large number of the electrons travel considerably off axis, because of finite transverse beam dimensions, initial beam velocity spreads, and injection with the beam centroid off axis.[5–15] For such off-axis electrons, the above approximate field is no longer adequate, and a more accurate description must be employed. Assuming—in good agreement with realized designs—that in the region of interest the magnetic field is uniform in one transverse direction (wide enough poles in the x direction in Fig. 1), the remaining two-dimensional magnetic field, in order to satisfy Maxwell's equations, necessarily varies in the other transverse direction (y direction in Fig. 1), and exhibits axial field components outside the median plane (Fig. 2).[16] In addition to the rapid oscillations in the x-z plane that are already present with the unrealistic one-dimensional (1D) field, a realistic 2D field induces slow betatron oscillations in the y-z plane,[17–23] on which are superimposed small-amplitude rapid oscillations in the same plane.[21] The additional electron oscillations in realistic wiggler fields must be expected to affect the spectral and angular distributions of the emitted radiation, and some of the crucial phase relations in a FEL.

The off-axis electron trajectories in realistic 2D static magnetic fields have been calculated numerically, including undulator field errors[22] and fringing fields at the

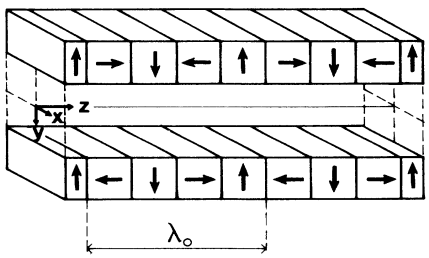

FIG. 1. Sketch of a two-period permanent wiggler with axis conventions shown.

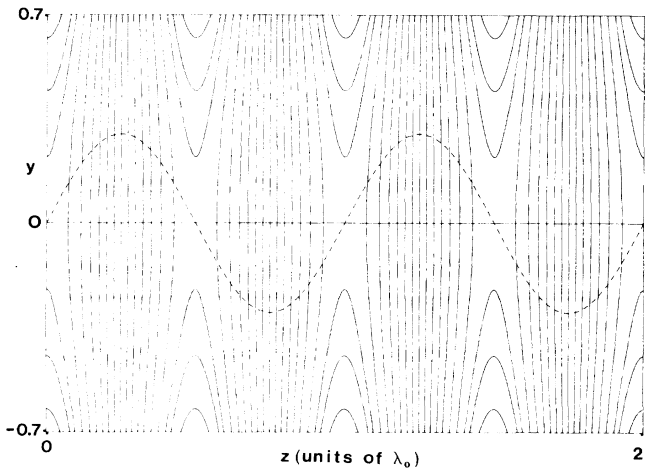

FIG. 2. Field lines, denoted by solid lines, of a 2D static magnetic field in the transverse y-z plane with a sinusoidal on-axis field variation, indicated by the dashed line.

wiggler ends.[23] However, *analytic* expressions for the single-electron trajectories are essential for several reasons. (a) One can hope to calculate the radiation pattern from a particular wiggler or undulator only if at least the electron velocity is given in a closed form;[24] (b) analytic expressions for single-electron trajectories give a better insight into the complicated dependence of the electron motion on parameters like the injection conditions at the wiggler entrance or the wiggler parameter K; (c) analytic single-particle trajectories are an essential starting point for investigating advanced problems such as stability analyses and FEL performance.

Therefore there has also been a great interest in finding the electron trajectories in analytic form.[18–21] One way to establish these is to exploit the two constants of the motion that exist in a 2D magnetic field of the above type, namely, the energy and the canonical momentum with respect to the uniform transverse direction. With their help the problem of finding analytic trajectories can essentially be reduced to the problem of solving in closed form a single complicated second-order ordinary differential equation, which governs the transverse motion in the y-z plane. In the case of a sinusoidal on-axis field variation, this transverse motion (assuming small transverse amplitudes) is often approximated by a simple harmonic oscillation. The approximation consists in averaging over the rapid oscillations and in taking into account only linear terms in a normalized transverse amplitude in the equation of motion, and essentially yields the above betatron oscillations.[18–21] Luccio and Krinsky give an analytic expression for the small-amplitude rapid oscillations that are superimposed on the slow betatron oscillations[21] again for a sinusoidal on-axis field variation, and taking into account only lowest-order terms in the transverse variable.

For electrons traveling considerably off axis, however, it is to be expected that analytic expressions[18–21] based only on the lowest-order terms in a normalized transverse variable are insufficient to describe the motion accurately. In fact, in many devices real transverse beam dimensions, initial beam velocity spreads,[5–14] lateral beam injection,[15] and a small undulator period λ_0 (Refs. 25–28) (note that the relevant off-axis scale is not the transverse amplitude y itself, but the ratio $2\pi y/\lambda_0$) lead to electrons traveling considerably off axis. For electron-beam sources supplying electron beams with transverse beam dimensions in the millimeter region, such as linacs,[5–9] electrostatic accelerators,[10] and microtrons,[11] the usual wiggler or undulator periods in the centimeter region lead to ratios $2\pi y/\lambda_0$ typically up to 0.6, i.e., extending into the far-off-axis regime. For small-period undulators with periods in the millimeter region, proposed in Refs. 25–28 to achieve shorter-wavelength undulator radiation with moderate energies, the off-axis scale $2\pi y/\lambda_0$ assumes values greater than 0.1 also for low emittance sources such as most storage rings,[12–14] which supply electron energies of hundreds of MeV with transverse beam dimensions of 0.05–1 mm. In the following analysis, we therefore include terms up to fifth order in the normalized transverse variable to achieve high accuracy also for far-off-axis trajectories.

As another important point we note that a purely sinusoidal on-axis field variation is only an approximation to the true magnetic field. Indeed, the fields of plane electromagnets or of permanent magnets in the Halbach configuration (Fig. 1) require for their description the inclusion of higher harmonics.[16,26] the transverse variation of which becomes progressively important for increasing distances from the wiggler axis. While for plane electromagnets and for Halbach configurations the harmonic content can be substantially taken account of by including second-harmonic terms,[16] higher harmonics seem to be of greater relevance for microundulators as proposed in Ref 26. Besides, in order to optimize the radiation characteristics from wigglers and undulators, efforts are being made to produce on-axis field variations that deliberately deviate from a sinusoidal form.[29] We thus strive in this paper for accurate analytic trajectories in realistic 2D magnetic fields with *arbitrarily* prescribed periodic on-axis field variation.

In Sec. II we define the class of static magnetic fields considered and derive the corresponding vector potential. With the aid of the two constants of the motion that this class of fields admit, we reduce in Sec. III the set of relativistic equations of motion to one complicated nonlinear second-order ordinary differential equation for the transverse coordinate $y(z)$. This equation holds for the class of vector potentials specified in Sec. II, and it turns out to be weakly nonlinear for realistic beam parameters and for realistic values of $\delta_w = K/\gamma$. To solve this equation, we employ in Sec. IV a two-level second-order two-scale analysis, by means of which an accurate description of the y-z motion is established. This description exhibits all the features that one expects to find in off-axis motion, such as small-amplitude rapid wiggler oscillations superimposed on large-amplitude slowly varying betatron oscillations. In Sec. V, we discuss the implementation of the initial conditions, and in Sec. VI, we use the expression found for $y(z)$ to determine the complete 3D trajectory in analytic form. In Sec. VII, we specialize to a sinusoidal on-axis field variation in order to compare our

approximate trajectory graphically with the result of a numerical integration and with that found from the simple harmonic approach. We find the accuracy of our trajectories to be excellent and greatly superior to the simple harmonic approach for a wide range of the parameters of the problem, especially so for electrons traveling considerably off axis.

II. TRANSVERSE 2D MAGNETIC FIELDS

We consider 2D magnetic fields of the form

$$\mathbf{B}=B_y(y,z)\mathbf{e}_y+B_z(y,z)\mathbf{e}_z \ , \tag{2.1}$$

uniform along $\mathbf{e}_x$, and with $\mathbf{e}_z$ pointing along the wiggler axis (Fig. 1). We assume the x-z plane to be the median plane of symmetry, in which the magnetic field is parallel to $\mathbf{e}_y$ and varies periodically along the wiggler axis $\mathbf{e}_z$. We prescribe the on-axis field by an arbitrary periodic function $B_{\rm ax}(z)$ with period λ_0,

$$B_y(y=0,z)=B_{\rm ax}(z), \quad B_z(y=0,z)=0 \ . \tag{2.2}$$

The complete magnetic field of the type (2.1) with on-axis variation (2.2) that satisfies Maxwell's equations *in vacuo*, $\nabla\times\mathbf{B}=0$ and $\nabla\cdot\mathbf{B}=0$, can be written as

$$\mathbf{B}=\mathrm{Re}\{B_{\rm ax}(z+iy)\}\mathbf{e}_y+\mathrm{Im}\{B_{\rm ax}(z+iy)\}\mathbf{e}_z \ . \tag{2.3}$$

For a sinusoidal on-axis field variation, the magnetic field (2.3) is indicated in Fig. 2.

The corresponding vector potential to (2.3) is

$$\mathbf{A}=A(y,z)\mathbf{e}_x=\mathrm{Re}\left\{\int B_{\rm ax}(\zeta)d\zeta\right\}\mathbf{e}_x \ , \tag{2.4}$$

where $\zeta=z+iy$ is an auxiliary complex variable. For convenience, the gauge has been chosen such that

$$\int_0^{\lambda_0} A(y=0,z)dz=0 \ . \tag{2.5}$$

In the following, we write the only component of the vector potential in the form

$$A(y,z)=A_0\alpha(y,z) \ , \tag{2.6}$$

where A_0 is the maximum on-axis amplitude of $A(y,z)$.

III. EQUATIONS OF MOTION

If radiation reaction is left out of account, the relativistic single-electron trajectories in the class of magnetic fields considered are the solutions of the equation of motion (in the usual notation),

$$\frac{d}{dt}(\gamma\boldsymbol{\beta})=\frac{e}{m}\boldsymbol{\beta}\times\mathbf{B} \ . \tag{3.1}$$

The corresponding total energy,

$$E=mc^2\gamma_0 \ , \tag{3.2a}$$

is a constant of the motion, and, in magnetic fields of the type (2.1), also the x component of the canonical momentum,

$$p_x(z)=mc\gamma_0\beta_x(z)+eA_0\alpha(y,z)=p_{0x} \ , \tag{3.2b}$$

is a constant of the motion.

In the following, it is convenient to transform the independent variable t to the axial variable z. Performing this transformation and exploiting the two constants of the motion (3.2a) and (3.2b), the three equations (3.1) can be decoupled for arbitrary field variations $\alpha(y,z)$. In particular, we thus find a nonlinear second-order ordinary differential equation governing the electron motion in the y-z plane,

$$\begin{aligned}\frac{d^2y}{dz^2}=\epsilon^2[b-\alpha(y,z)]&\left[\left(\frac{dy}{dz}\right)^2+1\right]\\ &\times\left[\frac{\partial\alpha}{\partial y}(y,z)-\frac{dy}{dz}\frac{\partial\alpha}{\partial z}(y,z)\right]\\ &\times\{1-\epsilon^2[b-\alpha(y,z)]^2\}^{-1} \ ,\end{aligned} \tag{3.3}$$

where

$$\epsilon=\frac{\delta_w}{\beta_0}, \quad b=\frac{p_{0x}}{mc\gamma_0\delta_w} \ , \tag{3.4}$$

and where δ_w denotes as usual the wiggler parameter K divided by γ_0,

$$\delta_w=\frac{K}{\gamma_0}=\frac{eA_0}{mc\gamma_0} \ . \tag{3.5}$$

In order to simplify the notation, y and z denote from now on dimensionless variables that are obtained from the original variables y and z by multiplying them by $k_0=2\pi/\lambda_0$. Thus the new variables y and z are normalized to the wiggler period λ_0.

Since for all realistic wigglers and undulators the quantity δ_w, and, therefore, ϵ is small (typically a few parts in one hundred or less), Eq. (3.3) is weakly nonlinear. Since, furthermore, realistic beam parameters and field geometries limit the value of y to, say, $|y|\le 0.6$, the reduced potential $\alpha(y,z)$ and its derivatives may be expanded around $y=0$ in powers of y to an appropriate order. In the subsequent analysis, we will find the inclusion of terms up to $O(y^5)$ sufficient to ascertain the required accuracy even for far-off-axis motion.

IV. TWO-SCALE ANALYSIS

We attempt to establish an accurate periodic approximation to the solution of the weakly nonlinear equation (3.3), valid throughout the entire wiggler, by way of a two-scale perturbation analysis.[30–34] Therefore we introduce a "fast" scale z^+, associated with the wiggler period, and a "slow" one z^-, associated with the slow betatron oscillations. We take

$$z^+=z, \quad z^-=\epsilon z \ , \tag{4.1}$$

and, in the spirit of the two-scale approach, we treat z^+ and z^- as independent variables, such that

$$\begin{aligned}\frac{d}{dz}&=\frac{\partial}{\partial z^+}+\epsilon\frac{\partial}{\partial z^-} \ ,\\ \frac{d^2}{dz^2}&=\frac{\partial^2}{\partial z^{+2}}+2\epsilon\frac{\partial^2}{\partial z^+\partial z^-}+\epsilon^2\frac{\partial^2}{\partial z^{-2}} \ .\end{aligned} \tag{4.2}$$

We assume the solution in the form of an expansion,

$$y(z)=y_0(z^+,z^-)+\epsilon y_1(z^+,z^-)+\epsilon^2 y_2(z^+,z^-) +\epsilon^3 y_3(z^+,z^-)+\epsilon^4 y_4(z^+,z^-) . \tag{4.3}$$

Next we insert (4.1)–(4.3) into Eq. (3.3), after $a(y,z)$ and its derivatives have been expanded with respect to y, and equate coefficients of like powers in ϵ on both sides of the resulting equation. For ϵ^0 and ϵ^1 we find

$$\frac{\partial^2 y_0}{\partial z^{+2}}=0 \tag{4.4a}$$

and

$$\frac{\partial^2 y_1}{\partial z^{+2}}+\frac{\partial^2 y_0}{\partial z^+\partial z^-}=0 . \tag{4.4b}$$

In order to avoid secular terms in z^+, we see from (4.4a) that y_0 must depend only on the slow scale z^-,

$$y_0=y_0(z^-) . \tag{4.5}$$

Substituting this result into (4.4b), we find that also y_1 must depend only on the slow scale z^-,

$$y_1=y_1(z^-) . \tag{4.6}$$

As usual in two-scale procedures, the function $y_0(z^-)$ is determined by the requirement that $y_2(z^+,z^-)$ contain no secular terms in z^+. The equation that determines $y_2(z^+,z^-)$ is found from equating the coefficients of ϵ^2,

$$\frac{\partial^2 y_2}{\partial z^{+2}}=-\frac{\partial^2 y_0}{\partial z^{-2}}-f_1(z^+)y_0(z^-)-f_2(z^+)y_0(z^-)^3 -f_3(z^+)y_0(z^-)^5 , \tag{4.7}$$

where the $f_i(z^+)$ are periodic functions of the fast variable z^+, defined by

$$f_1=\left[a\frac{\partial^2 a}{\partial y^2}-b\frac{\partial^2 a}{\partial y^2}\right]_{y=0,\,z=z^+} , \tag{4.8a}$$

$$f_2=\frac{1}{6}\left[a\frac{\partial^4 a}{\partial y^4}+3\left[\frac{\partial^2 a}{\partial y^2}\right]^2-b\frac{\partial^4 a}{\partial y^4}\right]_{y=0,\,z=z^+} , \tag{4.8b}$$

$$f_3=\frac{1}{12}\left[-\frac{1}{10}b\frac{\partial^6 a}{\partial y^6} +\frac{1}{10}a\frac{\partial^6 a}{\partial y^6}+\frac{3}{2}\frac{\partial^2 a}{\partial y^2}\frac{\partial^4 a}{\partial y^4}\right]_{y=0,\,z=z^+} . \tag{4.8c}$$

Note that no odd derivatives of $a(y,z)$ with respect to y appear as a consequence of the properties of the 2D magnetic field (2.1). We now extract the mean values a_{0i} from the 2π-periodic functions $f_i(z^+)$,

$$f_i(z^+)=a_{0i}+\bar{f}_i(z^+) , \tag{4.9}$$

where

$$a_{0i}=\frac{1}{2\pi}\int_0^{2\pi} f_i(z^+)dz^+ . \tag{4.10}$$

Obviously, the constants a_{0i} and the term $-\partial^2 y_0/\partial z^{-2}$ would give rise to secularities in y_2 with respect to the fast scale z^+ upon a double quadrature of (4.7). To avoid these, we require

$$\frac{\partial^2 y_0}{\partial z^{-2}}+\sum_{n=1}^{3} a_{0i}y_0^{2i-1}(z^-)=0 , \tag{4.11}$$

which is the desired equation for y_0.

With the a_{0i} found, Eq. (4.11) could be immediately integrated once and then solved exactly in terms of elliptic functions. However, sufficiently accurate approximate solutions are preferable, since they are easier to handle and still maintain the high overall accuracy that we intend to achieve. For this reason we first reduce (4.11) to a more convenient form by rescaling the dependent and independent variables according to $\sqrt{a_{01}}z^-=\bar{z}$ and $y_0=(y_0)_{\max}\bar{y}_0$, where $(y_0)_{\max}$ is the maximum amplitude of the oscillation. Then (4.11) reads

$$\frac{\partial^2 \bar{y}_0}{\partial \bar{z}^2}+\bar{y}_0+\bar{\epsilon}\bar{y}_0^3+\bar{\epsilon}^2\alpha\bar{y}_0^5=0 ,$$
$$\bar{\epsilon}=\frac{a_{02}(y_0)_{\max}^2}{a_{01}} , \tag{4.12}$$
$$\alpha=\frac{a_{03}a_{01}}{a_{02}^2} .$$

If $\bar{\epsilon}\ll 1$ and $\alpha=O(1)$, Eq. (4.12) is weakly nonlinear and is amenable to the application of a separate two-scale analysis,[32–33] independent of the above two-scale procedure with respect to ϵ. It turns out that the two-scale solution[33] of (4.12) is very accurate even up to comparatively large $\bar{\epsilon}$, such as, e.g., $\bar{\epsilon}\approx 0.5$. This means that the requirement $\bar{\epsilon}\ll 1$ is not very stringent, and that Eq. (4.12) can be considered to be weakly nonlinear for almost all physically relevant field variations, which in turn determine the magnitude of the coefficients a_{0i}.

By integrating (4.7) subject to (4.11), we find

$$y_2(z^+,z^-)=y_{\text{wiggle}}(z^+,z^-)+g_2(z^-) =\sum_{i=1}^{3} y_0^{2i-1}(z^-)h_i(z^+)+g_2(z^-) =-\sum_{i=1}^{3} y_0^{2i-1}(z^-)\int_{c_i}^{z^+}(z^+-z)\bar{f}_i(z)dz +g_2(z^-) , \tag{4.13}$$

where the $\bar{f}_i(z^+)$ have been defined in (4.9), and the constants c_i have to be chosen such that no terms proportional to z^+ appear as a result of the integration. For most applications it will be sufficient to determine the lowest-order term $h_1(z^+)$, as y_2 enters the solution (4.3) only multiplied by ϵ^2.

The term $y_{\text{wiggle}}(z^+,z^-)$ in (4.13) describes fast, small-amplitude oscillations, that are superimposed on the large-amplitude, slowly varying betatron oscillations, which are essentially described by $y_0(z^-)$. The function $g_2(z^-)$ in (4.13) is an as yet undetermined function of the slow scale, which improves the description of the betatron oscillations. In order to obtain a complete second-

order solution (involving y_0, y_1, and y_2), it therefore remains to establish $g_2(z^-)$ and $y_1(z^-)$.

The function $y_1(z^-)$ is determined by requiring that $y_3(z^+,z^-)$, although itself omitted from the solution that we are aiming at, contain no secular terms in z^+. Considerations analogous to the determination of $y_0(z^-)$ lead to a homogeneous equation of Mathieu type for $y_1(z^-)$ corresponding to (4.11) for $y_0(z^-)$. As will be seen in Sec. V, the implementation of the initial conditions leads to $y_1(0)=0$ and $\partial y_1/\partial z^-(0)=0$, which, in view of the equation for y_1 being homogeneous, requires $y_1(z^-)$ to vanish for all z^-,

$$y_1(z^-)=0 \ . \tag{4.14}$$

The function $g_2(z^-)$ in (4.13) must be found from the requirement that $y_4(z^+,z^-)$ contain no terms that are secular on the fast scale z^+. As $g_2(z^-)$ varies only on the slow scale, and appears in the expansion (4.3) only as a term multiplied by ϵ^2, it suffices to determine $g_2(z^-)$ from the terms linear in y in the expansion of the reduced potential $a(z,y)$ and its derivatives. Together with (4.14), this facilitates collecting the terms that make up the equation for y_4, and it ensures that the equation for $g_2(z^-)$ simplifies substantially,

$$\frac{\partial^2 g_2}{\partial z^{-2}}(z^-)+a_{01}g_2(z^-)=a_{04}y_0(z^-) \ . \tag{4.15}$$

The function $y_0(z^-)$ is the already known solution of (4.11), a_{01} is the first of the constants (4.10), and the constant a_{04} is given by

$$a_{04}=\frac{1}{2\pi}\int_0^{2\pi} f_4(z^+)dz^+ \ . \tag{4.16}$$

with the 2π-periodic function $f_4(z^+)$ being

$$\begin{aligned} f_4(z^+)=&\left[b\frac{\partial^2 a}{\partial y^2}(0,z^+)-a(0,z^+)\frac{\partial^2 a}{\partial y^2}(0,z^+)\right]h_1(z^+) \\ &-\left[b\frac{\partial a}{\partial z}(0,z^+)-a(0,z^+)\frac{\partial a}{\partial z}(0,z^+)\right]\frac{\partial h_1(z^+)}{\partial z^+} \\ &+[b-a(0,z^+)]^3\frac{\partial^2 a}{\partial y^2}(0,z^+) \ . \end{aligned} \tag{4.17}$$

Note that $h_1(z^+)$ has already been determined in finding $y_2(z^+,z^-)$ from (4.13).

We note that Eq. (4.15) is that of an undamped harmonic oscillator driven close to resonance, since from Eq. (4.11) the frequency of the driving term $y_0(z^-)$ is close to the eigenfrequency $\omega_0=\sqrt{a_{01}}$ of the oscillator on the left-hand side of (4.15). Thus $g_2(z^-)$ will show a nearly secular behavior on the slow scale z^-. In contrast to a fast-scale secularity, which we have so far successfully avoided, such a slow-scale behavior of $g_2(z^-)$ not only poses no problems, but on the contrary ensures that $g_2(\epsilon z)$ multiplied by ϵ^2 corrects $y_0(\epsilon z)$ in such a way that the two terms together describe the slow betatron motion of the electron very accurately. Since by virtue of the weak nonlinearity of Eq. (4.11), its (approximate) solution $y_0(z^-)$ is given in closed from, Eq. (4.15) can also be solved in closed form.

Thus all terms of the desired accurate second-order closed-form expansion of $y(z)$ are known,

$$y(z)=[y_0(\epsilon z)+\epsilon^2 g_2(\epsilon z)]+[\epsilon^2 y_{\text{wiggle}}(z)] \ , \tag{4.18}$$

where $y_0(\epsilon z)$ and $\epsilon^2 g_2(\epsilon z)$ describe the large-amplitude, slowly varying betatron oscillations, and $\epsilon^2 y_{\text{wiggle}}$ accurately describes the superimposed rapid oscillations with a slowly varying envelope.

V. IMPLEMENTATION OF THE INITIAL CONDITIONS

Our next task is to subject $y(z)$ to the initial conditions, in order to assign values to the various integration constants. These initial conditions are

$$\begin{aligned} &y(z=0)=\bar{y}_0 \ , \\ &y'(z=0)=\frac{\beta_{0y}}{\beta_{0z}} \ , \end{aligned} \tag{5.1}$$

where $\bar{y}_0$ is the electron's vertical distance from the wiggler axis at the wiggler entrance, and β_{0y} and β_{0z} denote the initial velocities in the y and z directions, respectively. Hence the conditions to be satisfied by the expansion $y(z)$ are

$$\bar{y}_0=y_0(0,0)+\epsilon y_1(0,0)+\epsilon^2 y_2(0,0) \tag{5.2a}$$

and

$$\begin{aligned} \frac{\beta_{0y}}{\beta_{0z}}=&\epsilon\frac{\partial y_0}{\partial z^-}(0,0)+\epsilon^2\frac{\partial y_1}{\partial z^-}(0,0)+\epsilon^2\frac{\partial y_2}{\partial z^+}(0,0) \\ &+\epsilon^3\frac{\partial y_2}{\partial z^-}(0,0) \ , \end{aligned} \tag{5.2b}$$

where the properties (4.5) and (4.6) have been incorporated. Equations (5.2a) and (5.2b) involve more than two integration constants. In order to determine them uniquely by only two equations, further conditions have to be imposed. The question of how different choices of these conditions give rise to different accuracies of the resulting expansion is discussed in greater detail by way of a similar example in Ref. 34. Here we adopt a policy that was found to lead to very accurate results.[34] It consists in setting those terms on the right-hand sides of (5.2a) and (5.2b) equal to the given initial values on the left-hand sides of (5.2a) and (5.2b), respectively, that involve y_0, and in setting equal to zero terms involving y_1 and y_2, respectively,

$$\bar{y}_0=y_0(0,0), \quad \frac{1}{\epsilon}\frac{\beta_{0y}}{\beta_{0z}}=\frac{\partial y_0}{\partial z^-}(0,0) \ , \tag{5.3a}$$

$$0=y_1(0,0), \quad 0=\frac{\partial y_1}{\partial z^-}(0,0) \ , \tag{5.3b}$$

$$0=y_2(0,0), \quad 0=\frac{\partial y_2}{\partial z^+}(0,0)+\epsilon\frac{\partial y_2}{\partial z^-}(0,0) \ . \tag{5.3c}$$

Equations (5.3a) allow us to determine uniquely the two integration constants in y_0. In the case that y_0 itself has to be found through an auxiliary two-scale procedure,[33] it

may at first involve more than two integration constants, which in turn have to be reduced to just two by adopting a similar implementation policy *before* substituting y_0 into (5.3a).[34] Note that (5.3b) was already used in Sec. IV to find $y_1(z^+,z^-)\equiv 0$. Equations (5.3c) determine the integration constants in $g_2(z^-)$, as the other part of $y_2(z^+,z^-)$, namely, $y_{\text{wiggle}}(z^+,z^-)$, only contains integration constants via $y_0(z^-)$, which are at this stage already known from (5.3a).

VI. COMPLETE TRAJECTORY

In Secs. IV and V an accurate expansion for the transverse motion in the y-z plane has been established for the given initial conditions. With the aid of the two constants of the motion (3.2a) and (3.2b), we can now proceed to find analytic expressions for all three velocity components as a function of z,

$$\beta_x(z)=\frac{p_{0x}}{mc\gamma_0}-\delta_w a(y(z),z)\ , \tag{6.1a}$$

$$\beta_y(z)=\beta_z(z)\frac{dy(z)}{dz}\ , \tag{6.1b}$$

$$\beta_z(z)=\left[\frac{\beta_0^2-\beta_x^2(z)}{1+\left[\frac{dy}{dz}\right]^2}\right]^{1/2}\ , \tag{6.1c}$$

with $y(z)$ from (4.18). In keeping with the expansions with respect to δ_w and y that were invoked to find the analytic expression (4.18), we also expand $\beta_x(z)$ and $\beta_z(z)$ with respect to δ_w and y. Assuming, furthermore, that $\beta_{0x}\ll 1$, which is well satisfied in all wigglers and undulators, we find

$$\beta_x(z)\simeq\delta_w\left[b-a(0,z)-\frac{1}{2}\frac{\partial^2 a}{\partial y^2}(0,z)[y_0^2(\epsilon z)+2\epsilon^2 y_0^2(\epsilon z)h_1(z)+2\epsilon^2 y_o(\epsilon z)g_2(\epsilon z)]-\frac{1}{24}\frac{\partial^4 a}{\partial y^4}(0,z)y_0(\epsilon z)^4\right]\ , \tag{6.2a}$$

$$\beta_y(z)\simeq\delta_w\left[\{1-\tfrac{1}{2}\epsilon^2[b-a(0,z)]^2\}\frac{dy_0(\epsilon z)}{d(\epsilon z)}+\epsilon\frac{dy_{\text{wiggle}}(z)}{dz}+\epsilon^2\frac{dg_2(\epsilon z)}{d(\epsilon z)}\right]\ , \tag{6.2b}$$

$$\beta_z(z)\simeq\beta_0\left\{1-\tfrac{1}{2}\epsilon^2\left[[b-a(0,z)]^2-[b-a(0,z)]\frac{\partial^2 a(0,z)}{\partial y^2}y_0^2(\epsilon z)+\left[\frac{dy_0(\epsilon z)}{d(\epsilon z)}\right]^2\right]\right\}\ . \tag{6.2c}$$

In (6.2a), $h_1(z)$ is the fast-scale dependence of the lowest-order term of y_{wiggle} as defined in (4.13).

In order to establish the complete trajectory in the convenient form $t(z)$, $x(z)$, and $y(z)$, it remains to perform two quadratures [as $y(z)$ has already been determined],

$$x(z)=x_0+\int_0^z\frac{\beta_x(z')}{\beta_z(z')}dz'\ , \tag{6.3a}$$

$$t(z)=\int_0^z\frac{dz'}{c\beta_z(z')}\ , \tag{6.3b}$$

where the initial conditions $x(0)=x_0$ and $t(0)=0$ have already been implemented. These integral representations of $x(z)$ are acceptable for some applications, for example, for the asymptotic evaluation of the classical radiation integral[35] that determines the spectral and angular characteristics of the radiation emitted by an electron following the trajectory $t(z),x(z),y(z)$ in the wiggler or undulator.[24] Yet, for other applications, it is preferable to have analytic expressions not only for the velocity components (6.1a)–(6.1c) or (6.2a)–(6.2c), but also for $x(z)$ and $t(z)$. To establish them, we expand the integrands of (6.3a) and (6.3b) with respect to δ_w up to second order, and the reduced vector potential $a(y,z)$ with respect to y up to an appropriate order, as we did in finding the expansions (6.2a)–(6.2c) of the velocity components. This yields

$$\begin{aligned}\frac{\beta_x(z)}{\beta_z(z)}\simeq\frac{\delta_w}{\beta_0}\Bigg[&b-a(0,z)-\frac{1}{2}\frac{\partial^2 a}{\partial y^2}(0,z)[y_0^2(\epsilon z)+2\epsilon^2 y_0^2(\epsilon z)h_1(z)+2\epsilon^2 y_0(\epsilon z)g_2(\epsilon z)]\\&-\frac{1}{24}\frac{\partial^4 a}{\partial y^4}(0,z)y_0(\epsilon z)^4+\tfrac{1}{2}\epsilon^2[b-a(0,z)]\left[\frac{dy_0(\epsilon z)}{d(\epsilon z)}\right]^2+\tfrac{1}{2}\epsilon^2[b-a(0,z)]^3\\&-\tfrac{1}{2}\epsilon^2[b-a(0,a)]^2\frac{\partial^2 a}{\partial y^2}(0,z)y_0^2(\epsilon z)-\tfrac{1}{4}\epsilon^2\frac{\partial^2 a}{\partial y^2}(0,z)[b-a(0,z)]^2y_0^2(\epsilon z)\Bigg]\ ,\end{aligned} \tag{6.4a}$$

$$\frac{1}{c\beta_z(z)}\simeq\frac{1}{c\beta_0}\left\{1+\tfrac{1}{2}\epsilon^2\left[[b-a(0,z)]^2-[b-a(0,z)]\frac{\partial^2}{\partial y^2}(0,z)y_0^2(\epsilon z)+\left[\frac{dy_0(\epsilon z)}{d(\epsilon z)}\right]^2\right]\right\}\ . \tag{6.4b}$$

With these expressions, the integrations in (6.3a) and (6.3b) only involve the known z dependence of the reduced potential α and its derivatives, and powers of the function $y(z)$, which is known in closed form. This allows us to calculate the expansions of $x(z)$ and $t(z)$ in closed form for a large number of physically relevant field variations $\alpha(y,z)$ by integrating (6.4a) and (6.4b) term by term.

VII. ANALYTIC VERSUS NUMERICAL SOLUTION

In order to assess the accuracy of the analytic approximation to the true trajectory $\mathbf{x}(z)$, and to compare this accuracy with the one achieved on the basis of the frequently employed simple harmonic oscillation in the y-z plane, we choose the example of a sinusoidal on-axis field variation. Using (2.4) and (2.5), such a sinusoidal on-axis field variation is described in (scaled variables) by a reduced vector potential of

$$\alpha(y,z)=\cosh(y)\cos(z) \ . \tag{7.1}$$

The corresponding constants a_{0i} [defined in (4.10)] are

$$a_{01}=\tfrac{1}{2}, \quad a_{02}=\tfrac{1}{3}, \quad a_{03}=\tfrac{1}{15}, \quad a_{04}=-\tfrac{3}{2}b^2-\tfrac{11}{32} \ . \tag{7.2}$$

With these constants, Eq. (4.12) can be accurately solved by an auxiliary two-scale procedure to yield[33]

$$\begin{aligned} y_0(\epsilon z)=&(a_0+a_1)\cos(\nu\epsilon z)+(b_0+b_1)\sin(\nu\epsilon z) \\ &+\tfrac{1}{48}a_0(a_0^2-3b_0^2)\cos(3\nu\epsilon z) \\ &+\tfrac{1}{48}b_0(3a_0^2-b_0^2)\sin(3\nu\epsilon z) \ , \end{aligned} \tag{7.3}$$

with the "frequency" ν being given by

$$\nu=\frac{1}{\sqrt{2}}[1+\tfrac{1}{4}(a_0^2+b_0^2)+\tfrac{1}{64}(a_0^2+b_0^2)^2+\tfrac{1}{2}(a_0a_1+b_0b_1)] \ . \tag{7.4}$$

By virtue of its two-scale origin, $y_0(\epsilon z)$ involves four integration constants a_0, b_0, a_1, and b_1. The two equations (5.3a), to which $y_0(\epsilon z)$ has to be subjected, place only two conditions on these four constants. Therefore a policy such as the one in Ref. 34 has to be adopted to determine all four of them. Carrying out the integrations in (4.13), we find

$$\begin{aligned} y_{\text{wiggle}}(z)=&-b\cos(z)[y_0(\epsilon z)+\tfrac{1}{6}y_0(\epsilon z)^3+\tfrac{1}{120}y_0(\epsilon z)^5] \\ &+\tfrac{1}{8}\cos(2z)[y_0(\epsilon z)+\tfrac{2}{3}y_0(\epsilon z)^3+\tfrac{2}{15}y_0(\epsilon z)^5] \ . \end{aligned} \tag{7.5}$$

The function $g_2(\epsilon z)$ can be easily found from (4.15), which can be solved exactly for the values of a_{01} and a_{04} given by (7.2), and for the driving term $y_0(\epsilon z)$ given by (7.3). Inserting (7.3), (7.4), and $g_2(\epsilon z)$ into (4.18) yields the desired expansion $y(z)$ in closed form.

We begin our comparative studies with the $y(z)$ motion. Off-axis injection as well as initial velocity spread give rise to an oscillating motion in the y-z plane, in addition to the large-amplitude oscillation in the x-z plane. The y-z motion consists of small-amplitude, rapid oscillations superimposed on a large-amplitude, slowly varying betatron motion. This betatron motion, accurately described by the terms $y_0(\epsilon z)+\epsilon^2 g_2(\epsilon z)$ in (4.18), is shown in Fig. 3 for two different sets of initial conditions. It can be seen that the electrons perform about one full betatron oscillation in the relatively strong ($K=10$) 30-period wiggler chosen. For smaller values of K or higher injection energies, i.e., for a smaller value of δ_w, the wavelength of betatron motion increases, so that the electrons will reach the wiggler end before having completed a full betatron oscillation. This is the case in many realized devices.

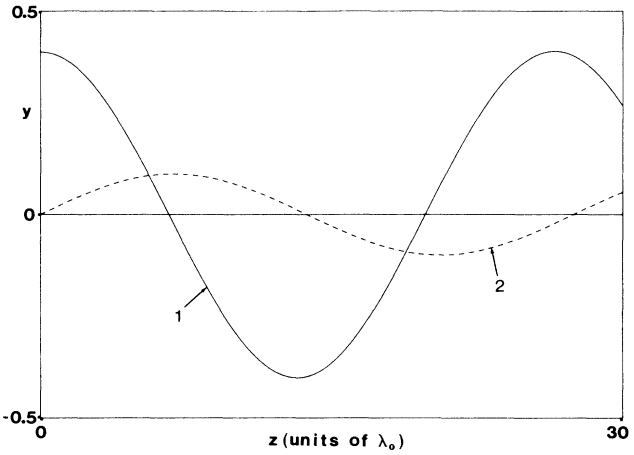

FIG. 3. Slow betatron oscillation in the y-z plane for two different sets of initial conditions: $\bar{y}_0=0.4$, $\beta_{0y}=0$ (solid curve 1), and $\bar{y}=0$, $\beta_{0y}/\beta_{0z}=3.6$ mrad (dashed curve 2), but otherwise identical parameters ($\beta_{0x}=0$, $\delta_w=0.05$, $\gamma_0=195$, $N_\beta=1{,}06$).

Besides a laterally displaced injection as in curve 1 of Fig. 3, also a realistic angular spread of the electron beam, that is a transverse velocity component β_{0y} at the wiggler entrance, leads to betatron oscillations of considerable amplitude, as indicated by the dashed curve 2 in Fig. 3. In fact, most electrons will enter the wiggler or undulator both at a transverse distance $\bar{y}_0$ from the wiggler axis and with a transverse velocity component β_{0y}.

In addition to the slow betatron motion (Fig. 3) in the y-z plane, the electrons execute rapid oscillations of small amplitude in the same plane, which are described by the term $\epsilon^2 y_{\text{wiggle}}(z)$ in (4.18). For better graphical display, $y_{\text{wiggle}}(z)$ is shown separately in Fig. 4, which—after multiplication by ϵ^2—should be imagined to be superimposed on curves 1 and 2 of Fig. 3, respectively.

Next, we compare, still for the case of sinusoidal on-axis field variation, the accuracy of our solution (4.18) with the accuracy achieved by the usual result in the near-axis regime, which arises from considering only terms of lowest order in y and from averaging over the rapid oscillations. This usual result is a simple harmonic oscillation,[18–21] which after implementation of the initial conditions (5.1) reads

$$y_{\text{harmonic}}(z)=\bar{y}_0\cos\left[\frac{\delta_w z}{\sqrt{2}}\right]+\frac{\beta_{0y}\sqrt{2}}{\beta_{0z}\delta_w}\sin\left[\frac{\delta_w z}{\sqrt{2}}\right] \ . \tag{7.6}$$

In Fig. 5 we compare the relative deviations Δ_y of our

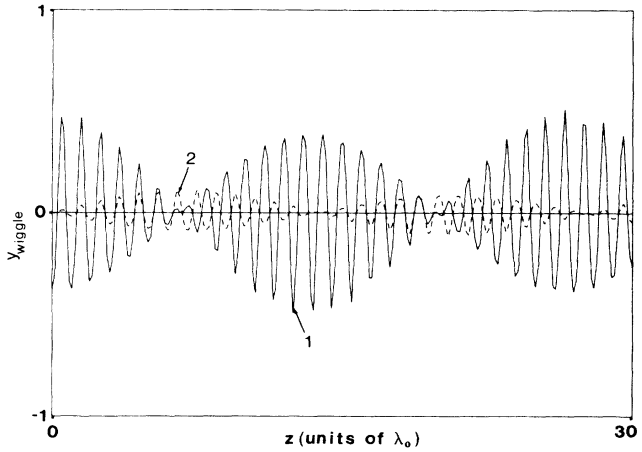

FIG. 4. Behavior of the small-amplitude rapid oscillations in the y-z plane that are superimposed on the slow betatron oscillations shown in Fig. 3 for the same sets of parameters as in that figure.

solution (4.18) [with $y_0(\epsilon z)$ from (7.3) and $y_{\text{wiggle}}(z)$ from (7.5)], and of the harmonic solution (7.6) from an exact numerical solution of Eq. (3.3), with $\alpha(y,z)$ taken from (7.1). By *relative* deviation Δ_y we mean the differences between the respective approximate solutions (4.18) and (7.6), and the exact solution, divided by the maximum amplitude of the betatron motion, which is essentially equal to the maximum amplitude of the y-z motion. The parameters chosen in Fig. 5 correspond to the far-off-axis regime, i.e., maximum values of the normalized transverse variable of about 0.3 and above. Such values result from substantial initial transverse displacements of the electron entering the wiggler, in Fig. 5 about 4% of the wiggler period λ_0, and/or from a substantial initial transverse velocity spread, which is taken to be 11 mrad in Fig. 5. Indeed, a substantial portion of electrons supplied from electron sources such as linacs,[5–9] microtrons,[11] and electrostatic accelerators,[10] will travel so far off axis if a wiggler or undulator period in the usual centimeter region is used. Such a far-off-axis regime can even be relevant for low emittance sources such as storage rings,[12–14] if the wiggler period is in the millimeter region as proposed in Refs. 25–28.

Curve 2 of Fig. 5 shows that the relative deviation of the harmonic solution (7.6) exceeds 15% after as few as 20 wiggler periods, which corresponds to about $N_\beta=0.7$ betatron oscillations. In contrast, the solution (4.18) is much more accurate, with typical relative deviations of a few parts in a thousand (dashed curve 1 in Fig. 5). We note that the high accuracy of the solution (4.18) is not only due to the inclusion of terms up to fifth order in the transverse variable, but also due to the inclusion of $\epsilon^2 g_2(\epsilon z)$ and $\epsilon^2 y_{\text{wiggle}}(z)$. The dashed curve 1 in this figure is the difference between (4.18) and the exact solution and its smooth behavior indicates that this difference does not vary on the fast scale, i.e., with individual wiggler periods, and, therefore, that (4.18) correctly describes the rapid oscillations in the y-z plane that are superimposed on the slow betatron motion. In contrast, curve 2 of Fig. 5 exhibits a fast oscillatory behavior, reflecting the fact that the harmonic solution (7.6) takes no account of these rapid oscillations.

Fig. 6 shows that also in the intermediate-off-axis regime, with a maximum transverse normalized amplitude of about 0.1, the analytic solution (4.18) is superior to the harmonic solution (7.6). Such transverse amplitudes typically occur with initial transverse displacements of about 1–2 % of the wiggler or undulator period, and with initial beam velocity spreads of a few mrad. This intermediate-off-axis regime is not only relevant for devices using electron sources with transverse beam dimensions in the millimeter region, but also for some low emittance sources, such as storage rings in the 100-MeV regime in combination with wiggler or undulator periods of up to a few centimeters. Note that the relative difference

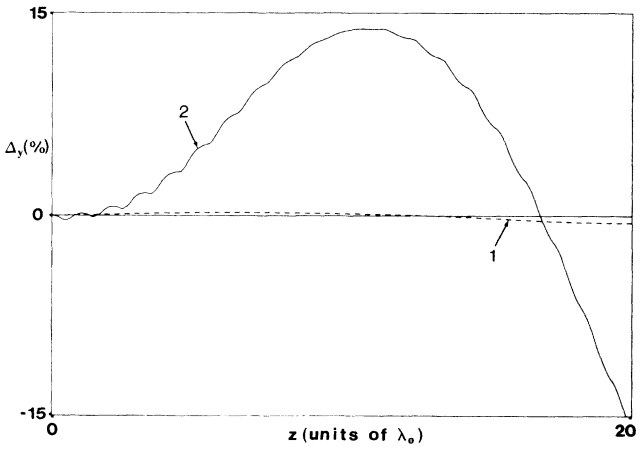

FIG. 5. Comparison of the relative deviations Δ_y of the solution (4.18) (dashed curve 1) and the simple harmonic solution (7.6) (solid curve 2) from the exact numerical solution of (3.3) for the y-z plane motion, in the far-off-axis regime ($\bar{y}_0=0.25$, $\beta_{0y}/\beta_{0z}=11$ mrad, $\beta_{0x}=0$, $\delta_w=0.05$, $\gamma_0=195$, $N_\beta=0.71$).

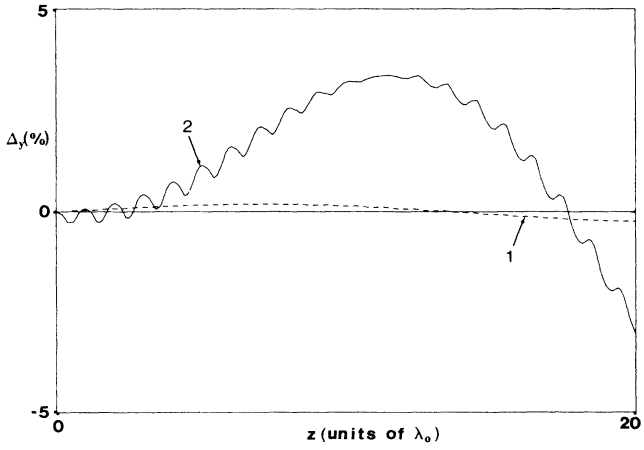

FIG. 6. Comparison of the relative deviations Δ_y of the solution (4.18) (dashed curve 1) and the simple harmonic solution (7.6) (solid curve 2) from the exact numerical solution of (3.3) for the y-z plane motion, in the intermediate-off-axis regime ($\bar{y}_0=0.08$, $\beta_{0y}/\beta_{0z}=4.5$ mrad, $\beta_{0x}=0$, $\delta_w=0.05$, $\gamma_0=195$, $N_\beta=0.71$).

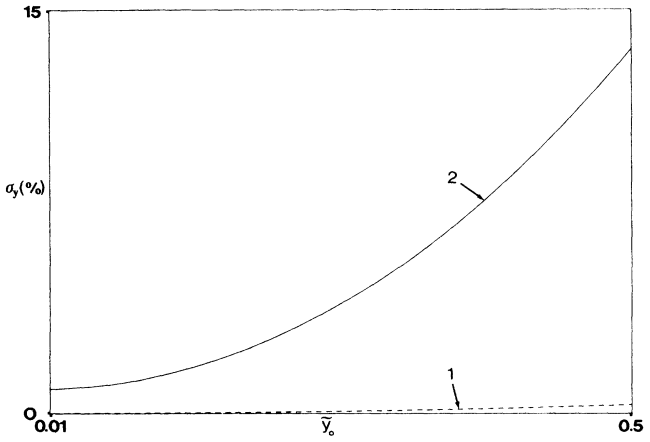

FIG. 7. Comparison of the mean relative deviations σ_y of the solution (4.18) (dashed curve 1) and the simple harmonic solution (7.6) (solid curve 2) from the exact numerical solution of (3.3) for the y-z plane motion. $\bar{y}_0$ is the initial displacement from the wiggler axis, the interval shown covering a range from near axis to far off axis ($\delta_w=0.05$, $\beta_{0y}=0$, $\beta_{0x}=0$, $\gamma_0=195$, $N=20$, $N_\beta=0.71$).

of the analytic solution (4.18) does not even oscillate on the enlarged scale of Fig. 6, reflecting the accurate description of the rapid oscillations by the term $\epsilon^2 y_{\text{wiggle}}(z)$ in (4.18).

In Figs. 7 and 8, we show the *mean* relative deviations σ_y, in order to study the dependence of the accuracies of (4.18) and (7.6) on various parameters, such as on the initial transverse electron distance from the wiggler axis (Fig. 7), or on the parameter δ_w (Fig. 8). For a given wiggler with a fixed number of periods, this quantity σ_y is obtained as usual by summing the squares of the relative deviations Δ_y^2 at n equidistant values of z, by dividing this sum by $n-1$, and by then taking the square root.

From Fig. 7 we see that the deviation σ_y of the harmonic solution (7.6) (curve 2) from the exact solution is substantial, especially in the far-off-axis regime, i.e., at the right end of the abscissa. In contrast, the accuracy of the solution (4.18) (dashed curve 1) remains high even in the far-off-axis regime, typically with mean relative deviations σ_y below a few parts in a thousand. Since in this figure the initial transverse velocity β_{0y} was taken to be equal to zero, the shown dependence of the mean relative deviation σ_y on the transverse injection displacement $\bar{y}_0$ is at the same time the dependence on the maximum transverse amplitude. This dependence hardly changes, if this maximum transverse amplitude is caused by a combination of transverse injection displacement $\bar{y}_0$ and transverse velocity component β_{0y}.

Figure 8 shows the dependence of the mean relative deviations σ_y on δ_w. This parameter essentially determines the frequency of the betatron oscillations in the y-z plane, and also the amplitude of the rapid oscillations superimposed on these betatron oscillations. As can be seen, for small values of δ_w the mean relative deviation σ_y of the harmonic solution (7.6) (solid curve 2) is only a few parts in one hundred and it is nearly zero for the analytical solution (4.18) (dashed curve 1). Such a behavior is to be expected, since the number of betatron oscillations N_β decreases with decreasing δ_w, and with almost no betatron oscillations ($N_\beta=0.07$ at the left end of the abscissa in Fig. 8), the solution (7.6) is nearly as satisfactory as (4.18).

The y-z motion studied so far in this section enters the remaining quantities $\beta_x(z)$, $\beta_z(z)$, $x(z)$ and $t(z)$ that constitute the complete trajectory, and errors in $y(z)$ therefore propagate to these quantities. In Fig. 9 we chose to study this error propagation by way of the relative deviations Δ_{β_x} of the velocity component β_x in the x-z plane

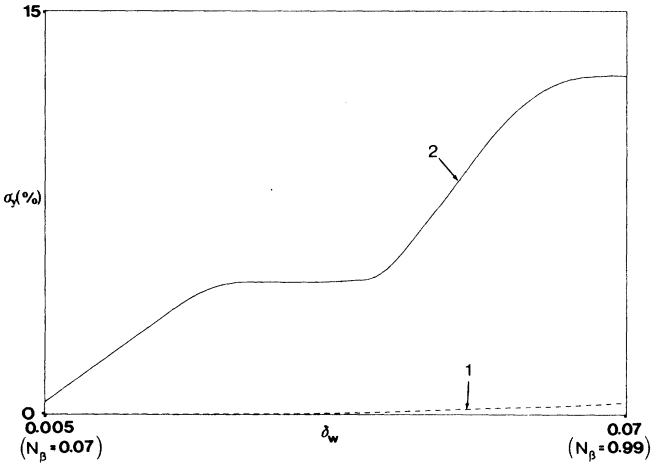

FIG. 8. Comparison of the mean relative deviations σ_y of the solution (4.18) (dashed curve 1) and the simple harmonic solution (7.6) (solid curve 2) from the exact numerical solution of (3.3) for the y-z plane motion, for fixed initial conditions ($\bar{y}_0=0.4$, $\beta_{0y}=0$, $\beta_{0x}=0$, $\gamma_0=195$, $N=20$), and as a function of δ_w.

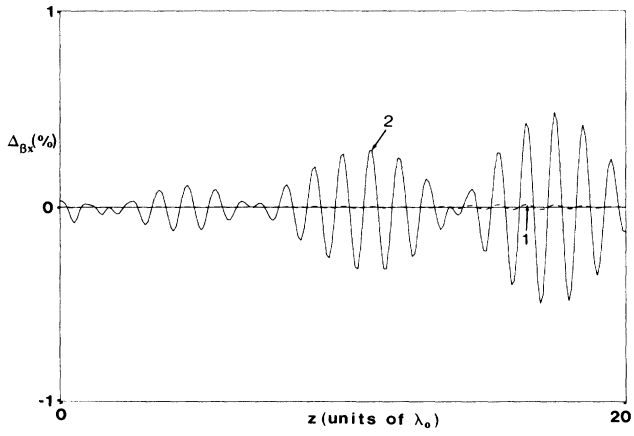

FIG. 9. Comparison of the relative deviations Δ_{β_x} of the velocity components in the x-z plane corresponding to (3.18) (dashed curve 1), and corresponding to the simple harmonic solution (7.6) (solid curve 2), from the exact numerical solution ($\beta_{0x}=0$, $\bar{y}_0=0.3$, $\beta_{0y}=0$, $\delta_w=0.05$, $\gamma_0=195$).

(*relative* meaning here that the differences of the approximate analytic solution for β_x from the exact solution are divided by δ_w, since the magnitude of this parameter is of the order of the amplitude of β_x). If β_x is calculated from the harmonic solution (7.6), we find Δ_{β_x} to lie below 1% even in the far-off-axis regime (solid curve 2 in Fig. 9), although the relative deviation Δ_y of (7.6) was typically 10% and more in the far-off-axis regime. As can be seen from the dashed curve 1 in Fig. 9 the relative deviation of β_x is nearly zero, if β_x (6.2a) is based on the analytic solution (4.18).

VIII. CONCLUSIONS

Since the usual magnetic field variation studied in the literature is the purely sinusoidal one, it was obvious to compare our approximate trajectory with that found from the simple harmonic approach, on the one hand, and with the result of a numerical integration, on the other hand. This comparison revealed an excellent accuracy of our trajectories, which is greatly superior to the simple harmonic approach for a wide range of parameters, especially for those corresponding to electrons traveling in the intermediate- and far-off-axis regime (normalized transverse distance in the y-z plane from the wiggler axis about 0.1 and above). The high accuracy of our analytic solution in the off-axis regime, with its correct description of the rapid small-amplitude oscillations superimposed on the betatron oscillations, is to be considered an important feature, as, in fact, in many devices real transverse beam dimensions and initial beam velocity spreads, lateral beam injection, and a small undulator period λ_0 lead to electrons traveling considerably off axis.

Although not graphically represented in Sec. VII, our analytical trajectories also exhibit a high accuracy even outside the typical far-off-axis regime, that is, for normalized transverse distances from the wiggler axis greater than 0.6. This might be of interest if small-period undulators[25–28] are used with electron-beam sources that supply electron beams with transverse beam parameters leading to transverse amplitudes in the order of magnitude of the small undulator period, such as most linacs do.

Beyond the important accuracy considerations in Sec. VII and above, it should be noted that our approach is able to provide accurate analytic trajectories in realistic 2D magnetic fields with *arbitrarily* prescribed periodic on-axis field variation. This allows one to take into account field variations more realistic than the simple sinusoidal one, which might be of great relevance to microundulators,[26] and to on-axis field variations that deliberately deviate considerably from the sinusoidal one, as, for example, proposed in Ref. 29.

[1]D. F. Alferov, Yu. A. Bashmakov, and E. G. Bessonov, in *Proceedings of the Lebedev Physics Institute,* edited by N. G. Basov (Consultants Bureau, New York, 1976), Vol. 80, p. 97.

[2]A. N. Didenko, A. V. Kozhevnikov, A. F. Medvedev, M. M. Nikitin, and V. Ya. Epp, Zh. Eksp. Teor. Fiz. **76**, 1919 (1979) [Sov. Phys.—JETP **49**, 973 (1979)].

[3]S. Krinsky, Nucl. Instrum. Methods **172**, 73 (1980).

[4]B. M. Kincaid, J. Opt. Soc. Am. B **2**, 1294 (1985).

[5]C. W. Roberson, IEEE J. Quantum Electron. **QE-21**, 860 (1985).

[6]G. Saxon, Nucl. Instrum. Methods A **237**, 309 (1985).

[7]V. A. Polyakov and I. S. Shchedrin, Zh. Tekh. Fiz. **52**, 390 (1982) [Sov. Phys.—Tech. Phys. **27**, 250 (1982)].

[8]C. A. Brau, IEEE J. Quantum Electron. **QE-21**, 824 (1985).

[9]T. J. Orzechowski, E. T. Scharlemann, B. Anderson, V. K. Neil, W. M. Fawley, D. Prosnitz, S. M. Yarema, D. B. Hopkins, A. C. Paul, A. M. Sessler, and J. S. Wurtele, IEEE J. Quantum Electron. **QE-21**, 831 (1985).

[10]L. R. Elias, IEEE J. Quantum Electron. **QE-23**, 1470 (1987).

[11]E. D. Shaw, R. J. Chichester, and S. C. Chen, Nucl. Instrum. Methods A **250**, 44 (1986).

[12]E. E. Koch, D. E. Eastman, and Y. Farge, in *Handbook of Synchrotron Radiation,* edited by E. E. Koch (North-Holland, Amsterdam, 1983), Vol. 1, p. 1.

[13]M. Billardon, P. Ellaume, J. M. Ortega, C. Bazin, M. Bergher, M. Velghe, D. A. G. Deacon, and Y. Petroff, IEEE J. Quantum Electron. **QE-21**, 805 (1985).

[14]M. A. Preger, Nucl. Instrum. Methods A **237**, 343 (1985).

[15]J. A. Pasour and S. H. Gold, IEEE J. Quantum Electron. **QE-21**, 845 (1985).

[16]R. P. Walker, Nucl. Instrum. Methods A **237**, 366 (1985).

[17]T. S. F. Wang and R. K. Cooper, Nucl. Instrum. Methods A **250**, 138 (1986).

[18]T. J. Karr, Phys. Rev. A **35**, 1697 (1987).

[19]M. N. Rosenbluth, IEEE J. Quantum Electron. **QE-21**, 966 (1985).

[20]Cha-Mei Tang and P. Sprangle, in *Proceedings of the International Conference on Lasers, New Orleans, 1980,* edited by C. B. Collins (STS, McLean, VA, 1981), p. 13.

[21]A. Luccio and S. Krinsky, in *Free-Electron Generators of Coherent Radiation,* (Addison-Wesley, New York, 1982), p. 181.

[22]R. C. J. Hu and L. R. Elias, Nucl. Instrum. Methods A **250**, 120 (1986).

[23]K. M. Murray, IEEE J. Quantum Electron. **QE-21**, 1089 (1985).

[24]C. Leubner and H. Ritsch, Nucl. Instrum. Methods A **246**, 45 (1986).

[25]V. L. Granatstein, W. W. Destler, and I. D. Mayergoyz, Appl. Phys. Lett. **47**, 643 (1985).

[26]G. Ramian, L. Elias, and I. Kimel, Nucl. Instrum. Methods A **250**, 125 (1986).

[27]K. Halbach, in International Conference on Insertion Devices for Synchrotron Sources, Stanford, CA 1985, edited by R. Tatchyn and I. Lindau [Proc. Soc. Photo-Opt. Instrum. Eng. **582**, 68 (1986)].

[28]T. Meinander, in International Conference on Insertion Devices for Synchrotron Sources, Stanford, CA, 1985, edited by R. Tatchyn and I. Lindau [Proc. Soc. Photo-Opt. Instrum. Eng. **582**, 193 (1986)].

[29]N. A. Vinokurov, Nucl. Instrum. Methods A **246**, 105 (1986).

[30]J. A. Morrison, SIAM (Soc. Ind. Appl. Math.) Rev. **8**, 66 (1966).

[31]A. H. Nayfeh, *Introduction to Perturbation Techniques* (Wiley,

New York, 1981).
[32]J. Kevorkian and J. D. Cole, in *Perturbation Methods in Applied Mathematics,* Vol. 34 of *Applied Mathematical Sciences,* edited by S. John, J. P. LaSalle, and L. Sirovich (Springer, New York, 1981), Chap. 3.
[33]C. Leubner and P. Torggler, Applicable Anal. **26**, 161 (1987).
[34]P. Torggler and C. Leubner, Z. Angew. Math. Mech. (to be published).
[35]J. D. Jackson, in *Classical Electrodynamics* (Wiley, New York, 1975), Chap. 14.